ELSEVIER

Earth and Planetary Science Letters 165 (1999) 177–185

EPSL

Dyke propagation with distributed damage of the host rock

Catherine Mériaux [a,*], John R. Lister [b], Vladimir Lyakhovsky [a], Amotz Agnon [a]

[a] *Institute of Earth Sciences, The Hebrew University of Jerusalem, Givat Ram, Jerusalem 91904, Israel*
[b] *Institute of Theoretical Geophysics, Department of Applied Mathematics and Theoretical Physics, University of Cambridge, Silver Street, Cambridge CB3 9EW, UK*

Received 4 June 1998; revised version received 17 November 1998; accepted 22 November 1998

Abstract

Observations of off-plane inelastic deformation around dykes motivate consideration of models of fluid-driven crack propagation in a solid which can undergo material degradation, or damage. The application to dyke propagation of a recently proposed damage rheology [Lyakhovsky et al., J. Geophys. Res. 102 (1997) 27635–27649] based on thermodynamical principles and experimental measurements is discussed. The rate of accumulation of damage in this rheology is the product of a material-dependent parameter c_d and the square of the strain. For geological values, a dimensionless parameter $c_d\eta/\Delta P$ characterizing the ratio of a damage timescale to a flow timescale is very small, where η is the magmatic viscosity and ΔP the driving pressure. As a result, significant rates of damage are confined to a small region near the dyke tip, where the strain is large. Consideration of possible singularities in near-tip solutions, shows that the rate of propagation is governed by the viscous fluid mechanics. To a good approximation, the rate has a value equal to that given by the zero-stress-intensity solutions of previous models based on linear elastic fracture mechanics. Predictions from the damage rheology both of a narrow damage zone and of the rate of propagation are in good agreement with observations.

Keywords: dikes; propagation; damage; deformation; flow mechanism; cracks

1. Introduction

Study of magma-driven fractures or dykes has been motivated by abundant evidence from field observations and seismic signals that it is an important mechanism of magma transport in the lithosphere. However, a complete dynamic model is not yet available because the details of coupling between the viscous stresses, the country rock deformation and the micromechanics of fracture are not fully understood. The usual theoretical approach is based on linear elastic fracture mechanics (LEFM). Early solutions used fluid statics in an elastic cavity [1,2], though these have no natural timescale for propagation. More recent solutions considered the effects of viscous flow [3–9]. Estimates of the pressure scales [8] show that the general features and rates of magma-driven propagation are determined by the fluid mechanics. The mechanical resistance to fracture is argued to affect only the region near the propagating crack-tip and questions of crack initiation.

* Corresponding author. Present address: Institute of Theoretical Geophysics, Department of Applied Mathematics and Theoretical Physics, University of Cambridge, Silver Street, Cambridge CB3 9EW, UK. E-mail: meriaux@esc.cam.ac.uk

0012-821X/99/$ – see front matter
PII: S0012-821X(98)00264-7

The use of LEFM has been questioned for two reasons. First, inelastic deformation such as jointing and shear banding is observed to extend from tens of centimetres to tens of metres from eroded dykes (e.g. [10,11]). Thus, the assumption of a small process zone ahead of the crack tip could be wrong and laboratory measurements of fracture toughness may be misleading. Second, it has been argued theoretically that under large confining pressures there is no K-dominant region [12,13]. Both lines of argument suggest that more general models of deformation and fracture need to be developed to account for nonlinear and dissipative effects and to obtain a more accurate description of dyke propagation.

Recently, a model incorporating a damage rheology derived from thermodynamical principles and experimental measurements has been proposed to describe the mechanical response of rocks in various geological processes [14–17]. These authors have shown that the damage model can account realistically for many features associated with earthquakes and faults. Moreover, it has been proposed that such a damage model can provide a satisfactory description of crack propagation. The idea is that degradation of the material by damage ahead of the crack-tip reduces the elastic coefficients, the vanishing of the shear modulus leads to failure, and thus a description of crack propagation is obtained that accounts for off-plane inelastic deformation.

Here, we apply Lyakhovsky's damage rheology to the propagation of a magma-driven fracture. We consider the simple case of lateral propagation of a dyke in a two-dimensional framework. Focusing on the link between the damage model and a fracture criterion, we argue that, though propagation is due to critical damage at the dyke tip, the model predicts that the rate of propagation is determined by the fluid mechanics. We start by a brief presentation of the principles of the damage model and give the governing equations for propagation. An analysis of timescales and dimensionless groups follows. Finally, a discussion of the dynamic controls on propagation rate motivates a more specific analysis of the behaviour of the deformation at the crack tip and the effect of damage.

2. The damage model

We summarize here the main features of the damage model. Further explanation and motivation from experimental-sample tests are given in Lyakhovsky et al. [14]. The solid medium behaves as a damage-controlled nonlinear elastic material with elastic energy

$$U = \frac{1}{\rho}\left[\frac{\lambda}{2}I_1^2 + \mu I_2 - \gamma I_1\sqrt{I_2}\right] \tag{1}$$

where ρ is the density, and I_1, I_2 are the two invariants of the strain tensor e_{ij} defined by

$$I_1 = e_{ii} \tag{2}$$

$$I_2 = e_{ij}e_{ij} \tag{3}$$

The effects of damage are introduced by allowing the two Lamé coefficients $\mu(\alpha)$, $\lambda(\alpha)$ to depend on a local damage parameter α, and by the coupling coefficient $\gamma(\alpha)$, which also depends on α. Coupling vanishes, $\gamma = 0$, in undamaged material, $\alpha = 0$.

The energy U is associated with stresses

$$\sigma_{ij} = \rho\frac{\partial U}{\partial e_{ij}} = \left[\lambda(\alpha) - \frac{\gamma(\alpha)}{\xi}\right]e_{kk}\delta_{ij} + 2\left[\mu(\alpha) - \tfrac{1}{2}\gamma(\alpha)\xi\right]e_{ij} \tag{4}$$

where the dimensionless variable ξ, defined by

$$\xi = \frac{I_1}{I_2^{1/2}} = \frac{e_{ii}}{(e_{ij}e_{ij})^{1/2}} \tag{5}$$

describes the type of deformation (uniaxial strain, simple shear, etc.). For all deformations,

$$-\sqrt{3} \le \xi \le \sqrt{3}$$

Eq. 4 shows a linear stress–strain relation for a given type of deformation with effective elastic moduli that depend on the amount of damage α and the type of deformation ξ.

The amount of damage evolves with time as a result of the applied loading. The thermodynamic consideration of increasing entropy shows that the kinetics of the damage process is given by

$$\frac{\mathrm{d}\alpha}{\mathrm{d}t} = -c\frac{\partial U}{\partial \alpha} \tag{6}$$

where c is a positive coefficient [14].

The basic statement of the applied theory of damage is that a material is critically damaged, $\alpha = \alpha_{cr}$, when it does not support any load. Mathematically, this criterion corresponds to a loss of convexity of the elastic energy U. The critical damage α_{cr} depends on the invariant ξ of the deformation type and, consequently, on the type of loading. Loss of convexity of the elastic energy corresponds to failure of the material, or, interpreted in the present context, macroscopic fracture. The model is completed by constitutive equations for $\lambda(\alpha)$, $\mu(\alpha)$ and $\gamma(\alpha)$. It is argued in [14,16] that it is reasonable to assume that λ should be nearly independent of α and that μ and γ can be approximated by the linear forms $\mu = \mu_0 + \mu'\alpha$, $\gamma = \gamma'\alpha$. The damage parameter α can be scaled so that the maximum (over ξ) critical damage equals 1 and occurs when $\xi = \xi_0 \equiv \mu'/\gamma'$; the scaling $\alpha_{cr}(\xi_0) = 1$ determines μ' and γ' in terms of ξ_0. Eq. 6 for the evolution of damage then reduces to

$$\frac{d\alpha}{dt} = c_d I_2(\xi - \xi_0), \quad \text{for } \xi \geq \xi_0 \tag{7}$$

where c_d is a constitutive constant characterizing the rate of damage. The material parameters in Eq. 7 are estimated as $\xi_0 \approx -0.8$ and $c_d \approx 0.5$–$3\ s^{-1}$ from a variety of experimental measurements [14]. For $\xi < \xi_0$ (closer to isotropic compression), it is assumed that α either does not evolve or heals slowly. In this paper, we use the simplified model Eq. 7.

3. Scale analysis

Consider a fluid-filled crack embedded in an infinite elastic solid with the damage rheology described above. Suppose that the crack lies in a horizontal plane and let $l(t)$ be its length along the x-direction and $2h(x,t)$ its width (Fig. 1). Assume that the fluid is incompressible and has viscosity η. We consider only laminar flow. Let ΔP be a typical pressure scale such as the overpressure of the source of the fluid.

Given the rigidity μ_0 of the undamaged solid, it is expected that the deformation tensor $\mathbf{e}$ and the half-thickness h of the dyke will scale like

$$\mathbf{e} \propto \Delta P/\mu_0 \tag{8}$$

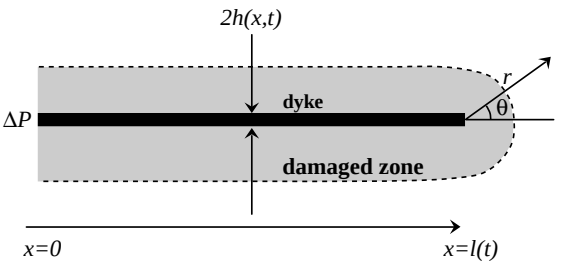

Fig. 1. Coordinate system and schematic model. A dyke of width $2h(x,t)$ extends from $x = 0$ to $x = l(t)$ driven by an overpressure ΔP of the source. Analysis of the near-tip solution is made using polar coordinates (r, θ) centred on the tip.

$$h \propto \Delta P l/\mu_0 \tag{9}$$

Three timescales are inherent in the problem, which can be found by non-dimensionalization of the time-derivative equations. An inertial timescale t_i is given by elastodynamics, whose general form is

$$\rho\frac{\partial^2 \mathbf{u}}{\partial t^2} = \nabla \cdot \boldsymbol{\sigma} + \rho\mathbf{g} \tag{10}$$

where $\mathbf{u}$ is the displacement vector, $\boldsymbol{\sigma}$ the stress tensor and $\mathbf{g}$ the acceleration due to gravity. The timescale for the damage t_d is derived from Eq. 7. The timescale for the viscous flow t_v is derived from the equation of mass conservation combined with Poiseuille flow:

$$\frac{\partial h}{\partial t} = \frac{1}{3\eta}\frac{\partial}{\partial x}\left(h^3\frac{\partial p}{\partial x}\right) \tag{11}$$

(e.g. [8,18]). Using Eqs. 7–11, we obtain

$$t_i = \left[\frac{\rho l^2}{\mu_0}\right]^{1/2} = \left[\frac{\mu_0}{\Delta P}\right]^2\left[\frac{\rho l^2 \Delta P^4}{\mu_0^5}\right]^{1/2} \tag{12}$$

$$t_d = \left[\frac{\mu_0}{\Delta P}\right]^2 \frac{1}{c_d} \tag{13}$$

$$t_v = \left[\frac{\mu_0}{\Delta P}\right]^2 \frac{\eta}{\Delta P} \tag{14}$$

The relative magnitude of these three timescales controls the dynamic regime of dyke propagation.

First, the inertial timescale is very short relative to the other two. For t_i to be larger than either t_v or t_d, the length of the dyke would need to satisfy either

$$l > l_1 = \left[\frac{\mu_0^5 \eta}{\rho \Delta P^5}\right]^{1/2} \tag{15}$$

or

$$l > l_2 = \left[\frac{\mu_0^5}{\rho c_d^2 \Delta P^4}\right]^{1/2} \quad (16)$$

Using some typical geophysical values (e.g. $\mu_0 \approx$ 10 GPa, $\eta \approx 100$ Pa s, $\Delta P \approx 1$ MPa, $\rho \approx 3000$ kg m^{-3}, $c_d \approx 0.5$ s^{-1}), we calculate $l_1 \approx 1.8 \times 10^9$ km and $l_2 \approx 1.8 \times 10^{11}$ km. We therefore conclude, as expected, that elastodynamic waves can travel from one end of the dyke to the other on a much shorter timescale than that of propagation. Thus, inertial acceleration can be neglected in Eq. 10 and the stresses found from elastostatics and the damage evolution.

The rate of propagation should thus be controlled either by t_d or by t_v. If $t_v \ll t_d$, the slower damage would be expected to control the dyke propagation rate and the fluid would thus be quasi-static. If $t_d \ll t_v$, the slower flow would be expected to control the propagation rate and there would be time for extensive damage around the dyke. A straightforward estimate of the two scales t_v and t_d with the values indicated above gives

$$\frac{t_v}{t_d} \approx \frac{\eta c_d}{\Delta P} \approx 10^{-4} \quad (17)$$

This shows that for geophysical parameters the timescale required for damage to evolve in the solid is much longer than the timescale associated with viscous flow. This suggests that propagating dykes should be damage-controlled.

As we shall show below, the previous approximation Eq. 13 of the damage timescale, which was based on an estimation of $I_2 = e_{ij}e_{ij}$ as being proportional to $[\Delta P/\mu_0]^2$ from Eq. 8, is not reliable in the region of the tip process zone, where $\mu \neq \mu_0$. The reason is twofold. First, we do not expect the stresses around the tip to be close to the source driving pressure ΔP in the dyke. Secondly, we expect the damage-controlled elastic coefficients to vary strongly in the region of the tip. In particular, the modulus of rigidity $\mu(\alpha)$ goes to zero towards the tip with the increase of damage. The timescale of damage in the tip region, which controls propagation of the tip, might thus be shorter than Eq. 13 suggests. These considerations motivate a closer examination of the stress, strain and damage fields near the tip.

4. Near-tip analysis of the effects of damage

As is well-known from LEFM, loading of the crack walls in an undamaged (uniform) elastic medium produces near-tip stress and strain singularities which vary like $r^{-1/2}$, where r is the distance from the tip. The purpose of this section is to examine the effect that damage, and the consequent variation of elastic coefficients, has on the strength of these singularities. We consider a plane-strain elastic problem with spatially varying elastic moduli. The general solution can be given in terms of an Airy stress function U, where

$$(M+N)\nabla^4 U + 2\nabla(M+N)\cdot\nabla\nabla^2 U + \nabla^2 N \nabla^2 U + \nabla\nabla M : \nabla\nabla U = 0 \quad (18)$$

and

$$M = \frac{1}{2\mu} \quad (19)$$

$$N = \frac{\lambda}{4\mu(\mu+\lambda)} \quad (20)$$

The derivations of a potential function U for the stress tensor from the equations of mechanical equilibrium and of Eq. 18 from the equations of strain compatibility are described in Appendix A.

We consider Eq. 18 in polar coordinates (r, θ) centred on the crack-tip, with the crack lying on $\theta = \pm\pi$. In order to obtain a definite problem, we assume that M and N take the form

$$M = r^a m(\theta) \quad (21)$$

$$N = r^a n(\theta) \quad (22)$$

Since we are concerned with the near-tip singularities, these forms can be thought of as the leading-order terms in an asymptotic expansion of the damage and moduli near the tip. Since the crack is associated with high damage, we expect $a \leq 0$ and $m(\theta)$, $n(\theta)$ to increase as θ varies from 0 to $\pm\pi$. We look for solutions to Eq. 18 the form

$$U = r^b f(\theta) \quad (23)$$

Substitution of Eqs. 21–23 into Eq. 18 leads to an equation of the form

$$L[f] = 0 \quad (24)$$

where L is a fourth-order linear differential operator with coefficients defined in terms of a, b, $m(\theta)$ and $n(\theta)$ (Appendix A). Eq. 24 is actually an eigenvalue equation for eigenvalues $b(a)$ and eigenfunctions $r^b f(\theta)$ of Eq. 18 subject to boundary conditions on the stresses.

In the (r, θ) plane, the stresses are given by

$$\boldsymbol{\sigma} = \begin{pmatrix} br^{(b-2)} f(\theta) + r^{(b-2)} f''(\theta) & -(b-1)r^{(b-2)} f'(\theta) \\ -(b-1)r^{(b-2)} f'(\theta) & b(b-1)r^{(b-2)} f(\theta) \end{pmatrix} \tag{25}$$

These stresses are symmetric about $\theta = 0$, since the damage can be taken to result in symmetric functions $m(\theta)$ and $n(\theta)$. It is assumed, as in LEFM, that the near-tip singularity is produced by distant loading of the crack walls and not by a singular loading distribution at the crack tip. Thus, $\sigma_{\theta\theta} = \sigma_{r\theta} = 0$ on the crack ($\theta = \pi$). From Eq. 25, the symmetry conditions at $\theta = 0$ and the loading conditions at $\theta = \pi$ give

$$f'(0) = 0 \tag{26}$$

$$f'''(0) = 0 \tag{27}$$

$$f(\pi) = 0 \tag{28}$$

$$f'(\pi) = 0 \tag{29}$$

The starting point for discussion is the familiar case of an uniform medium, which corresponds to $a = 0$ and m, n constant. For this case, it can be shown that equations Eq. 24 and Eqs. 26–29 have an eigensolution

$$f_0(\theta) = \cos^3\left(\frac{\theta}{2}\right), \quad b_0 = \tfrac{3}{2} \tag{30}$$

Since stresses vary like r^{b-2} and strains like r^{a+b-2}, this solution corresponds to a variation of both stresses and strains like $r^{-1/2}$. Indeed, this is just the near-tip solution for mode-I loading in LEFM.

Now, to investigate the effect of damage on the stress and strain singularities, we begin by applying a linear perturbation analysis. Supposing that

$$a = 0 + \delta a \tag{31}$$

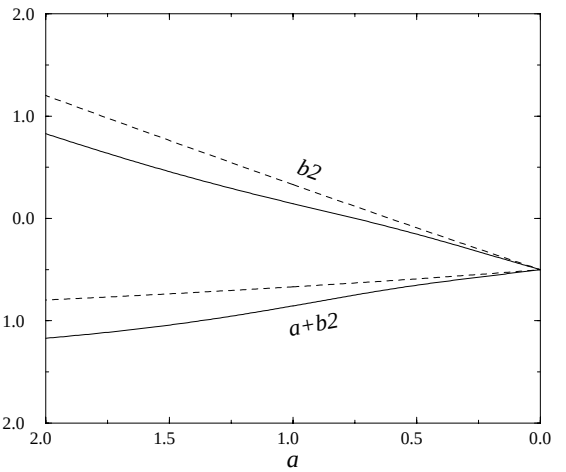

Fig. 2. The exponents $b-2$ and $a+b-2$ of the stress and strain singularities as a function of the exponent a parameterizing the strength of radial variation of damage (Eqs. 21 and 22). The solid lines correspond to the case of constant m and n; the dashed lines correspond to the case $m = n = [\cos(\theta/2)]^a$ which gives zero elastic moduli on the dyke plane $\theta = \pm\pi$.

$$b = b_0 + \delta b \tag{32}$$

$$f = f_0 + \delta f \tag{33}$$

where f_0 and b_0 are given by Eq. 30, we can show using standard techniques (Appendix A) that

$$\delta b = -\frac{5m + 6n}{8(m+n)}\delta a \tag{34}$$

Since $\delta a < 0$ in the case of interest, Eq. 34 implies, in particular, that $\delta b > 0$ and $\delta a + \delta b < 0$. Consequently, the effect of the damage ($\delta a < 0$) at the tip is a weaker singularity in the stresses but a stronger singularity in the strains. We checked Eq. 34 numerically and extended it beyond linear perturbations in a (Fig. 2). The stress relaxation ($b > b_0$) and crack-tip blunting ($a + b < b_0$) increases with the radial variation of damage (decreasing $a < 0$). We also considered by both perturbation and numerical methods the case of $m(\theta)$ and $n(\theta)$ increasing from $\theta = 0$ to $\theta = \pm\pi$, as envisaged for the near-tip damage field. With increasing variation in m and n, the solutions showed stress relaxation (increasing b) and crack-tip sharpening (increasing $a + b$), though these effects were weaker than those caused by variation of a.

These results from the near-tip analysis are important because they show that, while the stress

singularity at the tip can be regularized by damage relative to the linear elastic solution, the associated strain singularity is always increased by damage. In the following section, we analyse the implications of the behaviour found in the previous section for the establishment of a propagation criterion.

5. Discussion: propagation rates and criteria

We recall that material failure occurs at a critical damage $\alpha_{cr} \leq 1$ and, in the context of the present damage model, this must correspond to the criterion for crack extension: since the host rock has been assumed to have zero strength after failure, the invading magma front (or that of a tip cavity) must coincide with the point of failure. More general models in which failed material is assumed to have a granular or viscous rheology with non-negligible strength might allow magma propagation behind an envelope of failed material. However, since post-failure rheology is poorly constrained, we will not pursue such models further here.

We begin our discussion of the propagation rate by considering the evolution of damage around the tip in the frame of reference moving with the velocity **v** of the crack-tip. On a timescale less than l/v and a length scale less than l, both v and the damage distribution around the tip in this frame can be considered to be quasi-steady. Thus, Eq. 7 becomes

$$\mathbf{v} \cdot \nabla \alpha \propto c_d I_2 \tag{35}$$

which can be integrated to give

$$\alpha(r) \propto \frac{c_d}{v} \int_r^\infty I_2(r)\, dr \tag{36}$$

Let us first suppose that the dyke is propagating at a speed v of order l/t_d. Since $t_d \gg t_v$, the fluid is quasi-static and exerts a nearly constant pressure $\Delta P > 0$ along the dyke walls. This loading produces a near-tip strain singularity as discussed above. Now, the integral $\int_r^\infty I_2\, dr$ in Eq. 36 diverges as $r \to 0$ even in an undamaged LEFM solution. This divergence is even stronger in a solution accounting for damage ($a < 0$). Such a divergence implies that the rock reaches fracture ($\alpha = \alpha_{cr}$) some distance ahead of the tip. However, this contradicts the above hypothesis that the rate of extension v of the crack-tip is given by failure of material at the crack-tip. The fact that the rock is predicted to fail ahead of the crack-tip suggests that the dyke should be propagating faster than was first supposed. An increase in v does indeed alleviate the problem, since the right-hand side of Eq. 36 decreases and the point of failure moves closer to the dyke tip.

Let us now suppose that the propagation speed of the dyke is controlled by the fluid and hence that v is much larger and of order l/t_v. Significant damage would then occur only in a small region close to the tip where the large strains compensate for the small c_d/v. Outside of this region the deformation of the rock is well approximated by an undamaged linear-elastic solution. The coefficient of the I_2 singularity is determined by the distribution of pressure loading along the dyke, which is now affected by the pressure drop induced by viscous flow along the dyke. Owing to this pressure drop, I_2 will be less than in the earlier case of propagation on the damage timescale, in which quasi-static fluid exerts the source overpressure ΔP all along the dyke. In the context of LEFM, Spence and Sharp [18] derived a family of similarity solutions for fluid-driven propagation which was parameterized by the stress intensity at the tip. Solutions with larger rates of propagation correspond to smaller stress intensities, owing to the larger pressure drop and reduced loading, and there is a maximum rate of propagation at which the stress intensity is zero; thus weaker rocks allow rapid propagation as expected. In the present context, since the host-rock response is linear elastic except in the damaged tip region, the solutions will be very similar to those of Spence and Sharp and hence the dyke-wall loading is transmitted toward the tip region in the same way. Hence, while the response in the damaged tip region will be different, it is to be expected that the coefficient of the leading-order I_2 singularity will again decrease with increasing v and vanish at some limiting maximum velocity.

The two combined effects of an increase of v and a decrease of I_2 would substantially reduce $(c_d/v) \int_r^\infty I_2\, dr$, which suggests that an asymptotic solution can be obtained by matching Spence and Sharp's zero-stress-intensity solution for the propagation rate, fluid flow and external elastic response to a near-tip damage solution and a damaged 'bound-

ary-layer' left on either side of the dyke. By choosing v in this way, the leading-order singularity in I_2 can be eliminated by adjustment of the wall loading and only a lower-order singularity is left. In LEFM the $r^{-1/2}$ strain singularity for $K > 0$ is replaced when $K = 0$ by an $r^{-1/3}$ singularity if fluid occupies the tip or an $r^{1/2}$ singularity if there is a vapour-filled cavity [6,18]. Both of these weaker singularities give a convergent integral $\int_r^\infty I_2 \, dr$ as desired, though it should be noted that these second-order singularities will also be increased by damage.

While the above argument shows that v and the large-scale behaviour are given by the $K = 0$ solution of LEFM, it unfortunately does not identify the length scale l_d of the damage zone since the near-tip structure of the strain-field depends on the distribution of damage and vice versa. A rough order-of-magnitude estimate can be found by asking at what distance the timescale of damage $[d\alpha/dt]^{-1}$ is comparable to the timescale of propagation $l/v \approx t_v$ and (incorrectly) estimating $I_2 \approx (\Delta P/\mu_0)^2(l/l_d)$ from the $r^{-1/2}$ singularity for $K > 0$. Use of Eqs. 13, 14 and 36 then gives $l_d \approx (t_v/t_d)l = (c_d\eta/\Delta P)l$ or of order of a metre, which provides a first crude approximation to the scale of damage. It must be emphasized, though, that the damage affects the strain-field singularity and a proper estimate must await a fully coupled numerical simulation.

We have argued above that, in the present damage model, the requirement that damage reaches critical only at the crack-tip determines the propagation rate of a fluid-filled crack by adjustment of the viscous pressure drop, and thus gives realistic predictions for dyke propagation. It is interesting to note that application of a similar argument to a dry crack under tension, however small, would predict propagation at the dynamic crack velocity whereas either finite tensile strength or stress-corrosion cracking are observed. In the context of dry fracture other factors such as grain locking, heterogeneity and friction on the crack walls come into play, which have the effect of redistributing the stress singularity at the crack tip. Modelling of these phenomena requires elaboration of the damage model, for example, by the introduction of a nonlocal term to model finite-grain-size effects [19]. While investigation of such extensions is merited, the conclusion that dyke propagation is governed by the fluid timescale rather than the damage timescale must still hold by the independent argument that solidification is sufficiently rapid to rule out propagation on a damage timescale as unviable.

6. Conclusions

The present damage model reaffirms a fluid-controlled rate of propagation and points to a relatively narrow damage zone near the tip and on either side of the dyke. These predictions are in agreement with observations of dyke propagation at velocities of order 1 m s^{-1} and of off-plane damage extending a distance small in comparison to the dyke length.

Though we have presented analysis appropriate to an overpressure driven dyke, similar arguments hold for buoyancy-driven propagation. Thus, if the extent of damage is not of interest, the propagation of dykes and sills can be approximated by existing zero-stress-intensity solution in the framework of LEFM. It remains, of course, to perform a fully coupled calculation of flow, deformation and damage, and we note that the calculations here show that to be a non-trivial computational task since any numerical scheme will need both to resolve the narrow zone of damage and to calculate the large-scale elastohydrodynamic problem. Future more complicated models might include the effects of finite strain, nonlocal interactions and of anisotropy in the microstructural damage. For the moment, the agreement with observations noted above, together with the close similarity in predicted and observed geometries of shear banding around overlapping segments [11], is encouraging and provides strong motivation for further investigations of such models.

Acknowledgements

This study was made possible by generous grants from the Lady Davis Fellowship programme, the US–Israel Binational Science foundation and a TMR/Marie Curie Research Fellowship. We are very grateful to P. Delaney, R. Kerr and A. Rubin for thoughtful and constructive reviews of this manuscript and to G. Pijaudier-Cabot for useful discussions. ***[FA]***

Appendix A. Elastic solutions with variable moduli

Tensorial analysis can be used to solve an elastic problem in any system of coordinates. Two sets of equations are to be satisfied, namely the equations of equilibrium and the equations of compatibility. In a tensorial form, the stress tensor $\boldsymbol{\sigma}$ must satisfy the equilibrium condition

$$\nabla \cdot \boldsymbol{\sigma} = 0 \tag{37}$$

Eq. 37 implies in particular the existence of a second-rank potential tensor ψ such that

$$\boldsymbol{\sigma} = \nabla \wedge (\nabla \wedge \psi)^T \tag{38}$$

where T denotes transposition. The strain tensor $\mathbf{e}$, defined from the displacements $\mathbf{u}$ by

$$2\mathbf{e} = \nabla\mathbf{u} + (\nabla\mathbf{u})^T \tag{39}$$

has to satisfy the compatibility condition

$$\nabla \wedge (\nabla \wedge \mathbf{e})^T = 0 \tag{40}$$

In linear elasticity, stresses and strains are related by Hooke's law or its inverse:

$$\boldsymbol{\sigma} = 2\mu\mathbf{e} + \lambda \mathrm{tr}(\mathbf{e})\mathbf{I} \tag{41}$$

$$\mathbf{e} = \frac{1}{2\mu}\left(\boldsymbol{\sigma} - \frac{\lambda}{2\mu + 3\lambda}\mathrm{tr}(\boldsymbol{\sigma})\mathbf{I}\right) \tag{42}$$

where λ and μ are the elastic moduli, $\mathbf{I}$ is the identity tensor, and tr($\mathbf{e}$) and tr($\boldsymbol{\sigma}$) are the traces of the strain and stress tensors. In a plane-strain problem, with $\mathbf{k}$ the unit vector normal to the plane, the component e_{kk} of the strain tensor is zero. Hence, the potential tensor ψ can be written in terms of a potential scalar U, given by

$$\psi = \frac{1}{2(\lambda + \mu)}[(\lambda + 2\mu)\mathbf{kk} + \lambda\mathbf{I}]U \tag{43}$$

The stress tensor $\boldsymbol{\sigma}$ is then related to U by

$$\boldsymbol{\sigma} = \begin{pmatrix} \dfrac{\partial^2 U}{\partial x_2^2} & -\dfrac{\partial^2 U}{\partial x_1 \partial x_2} & 0 \\ -\dfrac{\partial^2 U}{\partial x_1 \partial x_2} & \dfrac{\partial^2 U}{\partial x_1^2} & 0 \\ 0 & 0 & \dfrac{\lambda}{2(\lambda+\mu)}\left(\dfrac{\partial^2 U}{\partial x_1^2} + \dfrac{\partial^2 U}{\partial x_2^2}\right) \end{pmatrix} \tag{44}$$

and the planar components can be expressed by

$$\boldsymbol{\sigma} = (\mathbf{k} \wedge \nabla)(\mathbf{k} \wedge \nabla)U \tag{45}$$

The compatibility equations Eq. 40 have only a **kk**-component, which can be written as

$$\nabla \cdot [\nabla \cdot (\mathbf{k} \wedge \mathbf{e} \wedge \mathbf{k})] = 0 \tag{46}$$

Equations Eqs. 42, 45 and 46 can be combined to give

$$\nabla \cdot [\nabla \cdot (M\nabla\nabla U) + \nabla \cdot \nabla \cdot (N\mathbf{I}\nabla^2 U)] = 0 \tag{47}$$

where M and N are given by Eqs. 21 and 22, and Eq. 47 can then be expanded to obtain Eq. 18. In the case of constant M and N, Eq. 47 gives the well-known biharmonic equation $\nabla^4 U = 0$.

In our analysis of the near-tip solution in a damaged medium, we considered the case where

$$M = r^a m(\theta) \tag{48}$$

$$N = r^a n(\theta) \tag{49}$$

and

$$U = r^b f(\theta) \tag{50}$$

Substitution into Eq. 47 gives

$$L[f] \equiv A_4(\theta) f^{(iv)} + A_3(\theta) f''' + A_2(\theta) f'' + A_1(\theta) f' + A_0(\theta) f = 0 \tag{51}$$

where the coefficient functions $A_i(\theta)$ are

$$A_4(\theta) = s(\theta) \tag{52}$$

$$A_3(\theta) = 2s'(\theta) \tag{53}$$

$$A_2(\theta) = s(\theta)(2b^2 - 4b + 4 + 2ab - 4a) + s''(\theta) + a(m(\theta) + an(\theta)) \tag{54}$$

$$A_1(\theta) = 2b^2 s'(\theta) + 2(1-a)(1-b)m'(\theta) \tag{55}$$

$$A_0(\theta) = s(\theta)b^2(b^2 - 4b + 4 + 2ab - 4a + a^2) + ab(2 - a - b)m(\theta) + bm''(\theta) + b^2 n''(\theta) \tag{56}$$

and $s(\theta) = m(\theta) + n(\theta)$.

The eigenfunctions f of L can be determined numerically or by a perturbation analysis about the eigenfunctions in LEFM. Linearization of Eq. 51 using Eqs. 31–33 and

$$L = L_0 + \delta L \tag{57}$$

where

$$L_0 = \frac{\partial^4}{\partial\theta^4} + \tfrac{5}{2}\frac{\partial^2}{\partial\theta^2} + \tfrac{9}{16} \tag{58}$$

and

$$\delta L = \delta a(m+n)\left[-\tfrac{3}{2} + 2\frac{\partial^2}{\partial\theta^2}\right] - \delta b\left(\tfrac{3}{2}m + n\right)\left[\tfrac{3}{2} + \frac{\partial^2}{\partial\theta^2}\right] \tag{59}$$

yields

$$L_0[\delta f] + \delta L[f_0] = 0 \tag{60}$$

where δf satisfies the same boundary conditions as f_0. The eigenvalue perturbation δb can then be calculated using an orthogonality relation. Integration by parts and use of the boundary conditions shows that

$$\int_0^\pi f_0 L_0[\delta f]\,\mathrm{d}\theta = \int_0^\pi \delta f L_0[f_0]\,\mathrm{d}\theta = 0 \tag{61}$$

It follows from Eqs. 60 and 61 that

$$\int_0^\pi f_0 \delta L[f_0]\,\mathrm{d}\theta = 0 \tag{62}$$

which can be used with Eqs. 30 and 59 to determine $\delta b(\delta a)$.

References

[1] J. Weertman, Theory of water-filled crevasses in glaciers applied to vertical magma transport beneath oceanic ridges, J. Geophys. Res. 76 (1971) 1171–1183.

[2] P.T. Delaney, D.D. Pollard, Deformation of host rocks and flow of magma during growth of Minette dikes and breccia-bearing intrusions near Shiprock, New Mexico, U.S. Geol. Surv. Prof. Pap. 1202, 1981, 61 pp.

[3] D.J. Stevenson, Migration of fluid-filled cracks: applications to terrestrial and icy bodies, Lunar Planet. Sci. Conf. 13th, 1982, pp. 768–769.

[4] D.A. Spence, D.L. Turcotte, Magma-driven propagation of cracks, J. Geophys. Res. 90 (1985) 575–580.

[5] D.A. Spence, P.W. Sharp, D.L. Turcotte, Buoyancy-driven crack propagation: a mechanism for magma migration, J. Fluid Mech. 174 (1987) 135–153.

[6] J.R. Lister, Buoyancy-driven fluid fracture: similarity solutions for the horizontal and vertical propagation of fluid-filled cracks, J. Fluid Mech. 217 (1990) 213–239.

[7] J.R. Lister, Buoyancy-driven fluid fracture: the effects of material toughness and of low viscosity precursors, J. Fluid Mech. 210 (1990) 263–280.

[8] J.R. Lister, R.C. Kerr, Fluid-mechanical models of crack propagation and their applications to magma-transport in dykes, J. Geophys. Res. 96 (1991) 10049–10077.

[9] A.M. Rubin, Propagation of magma-filled cracks, Annu. Rev. Earth Planet. Sci. 23 (1995) 287–336.

[10] P.T. Delaney, D.D. Pollard, J.I. Ziony, E.H. McKee, Field relations between dikes and joints: emplacement processes and paleostress analysis, J. Geophys. Res. 91 (1986) 4920–4938.

[11] R. Weinberger, G. Baer, G. Shamir, A. Agnon, Deformation bands associated with dyke propagation in porous sandstone, Makhtesh Ramon, Israel, in: Baer, Heimann (Eds.), Physics and Chemistry of Dykes, A.A. Balkema, Rotterdam, 1995, pp. 95–112.

[12] A.M. Rubin, Tensile fracture of rock at high confining pressure: implications for dike propagation, J. Geophys. Res. 98 (1993) 15919–15939.

[13] A.M. Rubin, Why geologists should avoid using 'fracture toughness' (at least for dykes), in: Baer, Heimann (Eds.), Physics and Chemistry of Dykes, A.A. Balkema, Rotterdam, 1995, pp. 53–63.

[14] V. Lyakhovsky, Y. Ben-Zion, A. Agnon, Distributed damage, faulting and friction, J. Geophys. Res. 102 (1997) 27635–27649.

[15] V. Lyakhovsky, Y. Podladchikov, A. Poliakov, Rheological model of a fractured solid, Tectonophysics 226 (1993) 187–198.

[16] A. Agnon, V. Lyakhovsky, Damage distribution and localization during dyke intrusion, in: Physics and Chemistry of Dykes, Baer, Heimann (Eds.), A.A. Balkema, Rotterdam, 1995, pp. 65–78.

[17] V. Lyakhovsky, Z. Reches, R. Weinberger, T.E. Scott, Nonlinear elastic behavior of damaged rocks, Geophys. J. Int. 130 (1997) 157–166.

[18] D.A. Spence, P.W. Sharp, Self-similar solutions for elastohydrodynamic cavity flow, Proc. R. Soc. London A 400 (1985) 289–313.

[19] J. Mazars, G. Pijaudier-Cabot, From damage to fracture mechanics and conversely: a combined approach, Int. J. Solids Struct. 33 (1996) 3327–3342.